B,N-Embedded Double Hetero[7]helicenes with Strong Chiroptical Responses in the Visible Light Region

Ji-Kun Li,[†] Xing-Yu Chen,[†] Yun-Long Guo,[‡] Xin-Chang Wang,[‡] Andrew C.-H. Sue,[‡] Xiao-Yu Cao,[‡] and Xiao-Ye Wang*[,†]

[†]State Key Laboratory of Elemento-Organic Chemistry, College of Chemistry, Nankai University, Tianjin 300071, China

[‡]College of Chemistry and Chemical Engineering, Xiamen University, Xiamen 361005, China

Abstract

The development of helicene molecules with significant chiroptical responses covering a broad range of the visible spectrum is highly desirable for chiral optoelectronic applications; however, their absorption dissymmetry factors (g_{abs}) have been mostly lower than 0.01. In this work, we report unprecedented B,N-embedded double hetero[7]helicenes with nonbonded B and N atoms, which exhibit excellent chiroptical properties, such as strong chiroptical activities from 300 to 700 nm, record high g_{abs} up to 0.033 in the visible spectral range, and tunable circularly polarized luminescence (CPL) from red to near-infrared regions (600 ~ 800 nm) with high photoluminescence quantum yields (PLQYs) up to 100%. As revealed by theoretical analyses, the high g_{abs} values are related to the separate molecular orbital distributions owing to the incorporation of nonbonded B and N atoms. The new type of B,N-embedded double heterohelicenes opens up an appealing avenue to the future exploitation of high-performance chiroptical materials.

Main Text

Helicenes are a unique class of inherently chiral polycyclic aromatic hydrocarbons (PAHs) comprising *ortho*-fused benzenoid rings. The development of helicene chemistry over the past century has promoted its broad applications in a variety of research fields.[1-6] Of particular interest is their potential as semiconducting materials for advanced chiral optoelectronic devices, such as circularly polarized light photodetectors,[7-8] for which strong chiroptical responses across a broad range of the visible spectrum are highly desirable.[9-10] However, most helicenes exhibit chiroptical activities mainly in the ultraviolet region,[11] thus calling for new design principles of helicene molecules. In recent years, enlarging the π-conjugated plane of helicenes and fusing multiple helicenes into a PAH core have led to a variety of elegant molecules that extend chiroptical responses to the visible spectral range.[12-29] Nevertheless, the absorption dissymmetry factors (g_{abs}) are generally in the range of 10^{-4} ~ 10^{-3},[30] with only very few compounds showing g_{abs} on the order of 10^{-2}.[12-17] Therefore, it is highly demanding to develop novel helicene materials with high g_{abs} in the visible range for future chiral optoelectronic applications.

Incorporating heteroatoms into the framework of helicenes and multiple helicenes provides new design strategies to modulate their chiroptical properties and offers new synthetic entries to such chiral materials.[31] Among various heterohelicenes and multiple heterohelicenes, only a few examples involving both boron (B) and nitrogen (N) atoms have been developed by employing either B-N covalent bonds or B→N coordinate bonds.[32-37] In view of the growing interest in B,N-doped PAHs as novel π-conjugated materials

with intriguing optoelectronic properties,[38-42] B,N-incorporated (multiple) heterohelicenes have seemingly been underexplored, with the reported g_{abs} only on the order of 10^{-3}.[33-35]

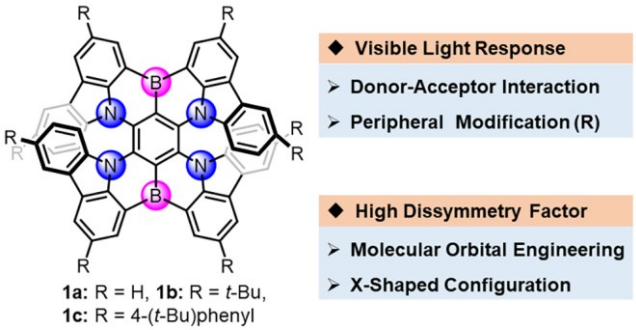

Figure 1. Molecular design of B,N-embedded double hetero[7]helicenes (**1a-c**) in this work.

Herein, we develop a new type of B,N-embedded double hetero[7]helicenes (**1a-c**) with nonbonded B and N atoms (Figure 1),[43] which exhibit excellent chiroptical properties. The *para*-conjugated N atoms (N-π-N) and B atoms (B-π-B) enhance the donor and acceptor strengths, respectively, leading to strong intramolecular donor-acceptor interactions and thus absorption of the visible light up to the red region.[42] The optical gap can be further lowered by attaching electron-donating groups. On the other hand, the opposite resonance effect of mutually *ortho*-positioned B and N atoms induces separate distribution of the molecular orbitals that are relevant to the optical transition.[44] Such a feature and the double helical X-shaped configuration have been demonstrated to be beneficial for achieving high g_{abs} values.[45-46] Remarkably, the obtained double hetero[7]helicenes (**1a-c**) exhibit significant chiroptical responses from ultraviolet to the whole visible regime (300 ~ 700 nm) with a maximum g_{abs} reaching 0.033 at 502 nm, representing the record high g_{abs} value in the visible range for helicene compounds. Furthermore, these double hetero[7]helicenes display tunable circularly polarized luminescence (CPL) from red to near-infrared (NIR) regions with high photoluminescence quantum yields (PLQYs) up to 100%. These excellent chiroptical properties demonstrate the high potential of B,N-embedded heterohelicenes as promising chiroptical materials and provides new opportunities for the future development of chiral optoelectronics.

Scheme 1. Synthetic route to B,N-embedded double hetero[7]helicenes 1a, 1b, and 1c.

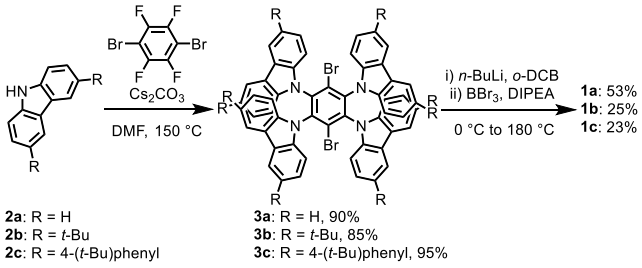

The synthetic route to compounds **1a-c** is depicted in Scheme 1. The corresponding precursors **3a-c** were synthesized through aromatic nucleophilic substitution reactions of 1,4-dibromotetrafluorobenzene with carbazole and its derivatives (**2a-c**) in 90%, 85% and 95% yields, respectively. Boron atoms were then introduced into the molecule through lithium-halogen exchange and subsequent nucleophilic substitution with boron tribromide. Finally, in the presence of *N*,*N*-diisopropylethylamine(DIPEA), intramolecular C-H borylation occurred at 180 °C in *o*-dichlorobenzene (*o*-DCB) to afford **1a-c** in 53%, 25% and 23% yields, respectively.

The single crystal of **1b** suitable for X-ray analysis was obtained by slow evaporation of its solution in dichloromethane/hexane (2 : 1). The double helical structure of **1b** was accurately confirmed by single-crystal X-ray diffraction, displaying overlaps between the terminal benzene rings (Figure 2). The torsion angles of the two hetero[7]helicene fragments were 24.30° (N1-C2-C3-N4) and 26.13° (N5-C6-C7-N8), respectively. The central benzene ring was highly distorted, with the torsion angles of 27.79° for C9-C2-C3-C10 and 29.62° for C9-C6-C7-C10. In the packing structure of **1b**, two enantiomers (*P*,*P* and *M*,*M*) were found, with the homochiral molecules packing along the *a*-axis. No obvious intermolecular π-π interaction was observed due to the existence of eight *tert*-butyl groups at the periphery of the skeleton. The (*P*,*M*)-configuration was not found in the single crystal of **1b**, in consistence with the NMR results.

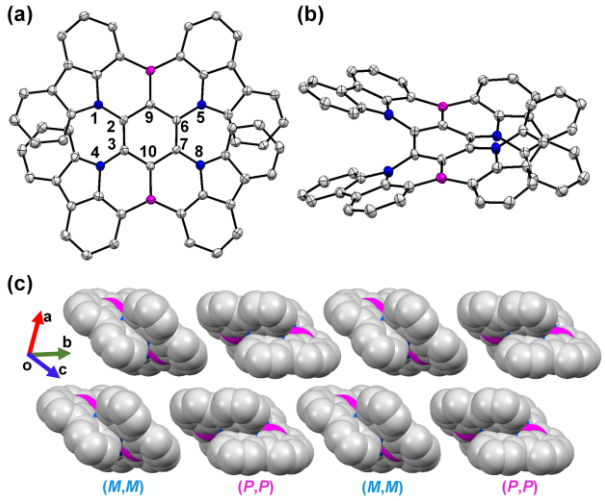

Figure 2. Single crystal structure of **1b**. (a) Top view and (b) side view. Thermal ellipsoids are shown at 50% probability. The *t*-Bu groups and hydrogen atoms are omitted for clarity. (c) Packing structure of **1b**.

The UV-vis absorption spectra of compounds **1a-c** were recorded in dichloromethane solutions (Figure S1a). The lowest-energy absorption maximum of **1a** appeared at 627 nm. With the attachment of *tert*-butyl and 4-(*tert*-butyl)phenyl substituents to the core, the corresponding absorption maxima of **1b** and **1c** red-shifted to 650 nm and 662 nm, respectively. The optical gaps calculated from the absorption onsets were gradually narrowed from 1.88 eV to 1.81 eV and 1.78 eV for **1a-c**. The electrochemical properties were investigated by cyclic voltammograms (CV) and differential pulse voltammograms (DPV). All three compounds **1a-c** exhibited two reversible oxidation waves and one reversible reduction wave. According to the DPV data, the lowest unoccupied molecular orbital (LUMO) energy levels of **1a-c** were determined to be -2.93 eV, -2.83 eV and -2.97 eV, while the highest occupied molecular orbital (HOMO) energy levels of **1a-c** were -4.94 eV, -4.75 eV and -4.89 eV, respectively (Figure S2).

Density functional theory (DFT) calculations were carried out to investigate the isomerization process of the double hetero[7]helicene skeleton (**1a**). The calculated energy barrier of the isomerization process was as high as 67.52 kcal/mol, indicating its excellent chiral stability (Figure S10). By using Daicel Chiralpak IE column for high-performance liquid chromatography (HPLC) analysis, two enantiomers (*P,P* and *M,M*) of each double hetero[7]helicene (**1a-c**) were identified (Figures S3-S5). Through chiral separation of the three compounds by preparative chiral HPLC, the enantiomers of each compound were successfully obtained. In order to verify the configurational stability of the enantiopure double hetero[7]helicenes, we heated the enantiomer **1a**-(*P*,*P*) in a furnace at 300 °C for 3 hours. The chiral HPLC

traces and NMR spectra before and after heating revealed no change (Figures S6 and S7), suggesting its high configurational stability, which laid the ground for further chiroptical characterizations.

As illustrated in Figure 3a, each pair of enantiomers (**1a-c**) displayed symmetric circular dichroism (CD) spectra with opposite Condon effects. The three compounds manifested similar CD features, but gradually red-shifted from **1a** to **1c**, indicating that the chiroptical properties could be modulated by the peripheral substituents. Note that the chiroptical responses of compounds **1a-c** covered the ultraviolet and the whole visible regions (300 ~ 700 nm), which is rare in the literature for helicene compounds.[30] The simulated CD spectra (Figure S12) were in good agreement with the experimental results, and indicated that for all the three compounds (**1a-c**), the first peak obtained by chiral HPLC was (*M*,*M*)-configuration, whereas the second peak was (*P*,*P*)-configuration. The g_{abs} values were calculated according to the equation $g_{abs} = \Delta\varepsilon/\varepsilon$, and the absolute $|g_{abs}|$ values were plotted as a function of wavelength (Figure 3b). The maximum $|g_{abs}|$ of **1a-c** reached 0.033, 0.031, and 0.026 at 502 nm, 518 nm, and 526 nm, respectively (Table 1), which represent the highest $|g_{abs}|$ values of helicene molecules in the visible range (Figure 3c).

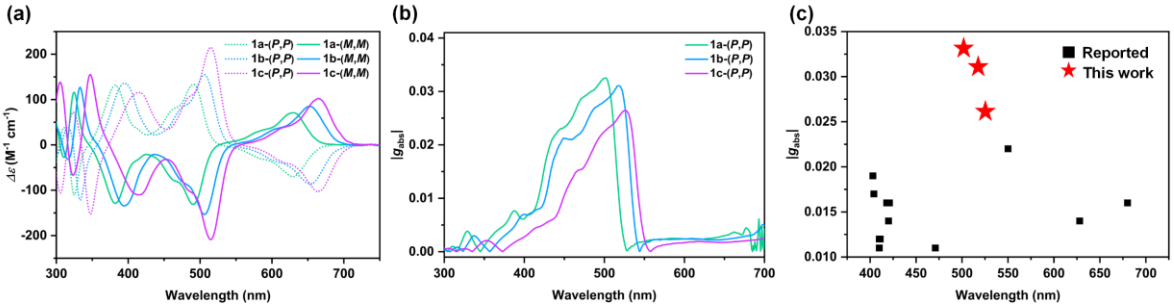

Figure 3. (a) Circular dichroism spectra of **1a-c** in dichloromethane solution (1×10^{-5} M), and (b) the corresponding $|g_{abs}|$ of (*P*,*P*)-configuration calculated according to the equation $g_{abs} = \Delta\varepsilon/\varepsilon$. (c) Summary of the $|g_{abs}|$ values of the reported helicenes and compounds **1a-c**. For more details, see the Supporting Information.

Table 1. Summary of the Chiroptical Properties of Compounds 1a-c.

compound	$\|g_{abs}\|$ S_1 / S_2	λ_{CD}[a] (nm) S_1 / S_2	$\|\boldsymbol{\mu}\|$[b] (10^{-18} esu cm) S_1 / S_2	$\|\boldsymbol{m}\|$[b] (10^{-20} erg G^{-1}) S_1 / S_2	θ[b] (deg) S_1 / S_2	$\|g_{cal}\|$[b] S_1 / S_2
1a	0.0025 / 0.033	587 / 502	5.52 / 1.67	0.46 / 2.65	0 / 180	0.0033/ 0.063
1b	0.0025 / 0.031	609 / 518	6.17 / 1.72	0.41 / 2.51	0 / 180	0.0027/ 0.058
1c	0.0019 / 0.026	619 / 526	7.36 / 2.41	0.41 / 2.60	0 / 180	0.0022/ 0.043

[a] The wavelength corresponding to the maximum $|g_{abs}|$ value. [b] Calculated by TD-DFT at the PBE0/6-311G(d) level.

To understand the origin of the high $|g_{abs}|$ values, time-dependent DFT (TD-DFT) calculations were performed at the PBE0/6-311G(d) level (see the Supporting Information). For all the three compounds (**1a-c**), the $S_0 \rightarrow S_1$ and $S_0 \rightarrow S_2$ transitions were contributed by HOMO→LUMO and HOMO→LUMO+1 transitions, respectively (Figure 4). The lowest-energy absorption peak was attributed to the $S_0 \rightarrow S_1$ transition, whereas the transition with the largest $|g_{abs}|$ was assigned to the $S_0 \rightarrow S_2$ transition. According to theory, the dissymmetry factors can be calculated by the equation $g = 4\cos\theta|\boldsymbol{m}||\boldsymbol{\mu}|/(|\boldsymbol{m}|^2+|\boldsymbol{\mu}|^2)$, wherein $\boldsymbol{\mu}$, $\boldsymbol{m}$, and θ represent the electric and magnetic transition dipole moments, as well as the angle between $\boldsymbol{\mu}$ and $\boldsymbol{m}$, respectively.[30] For small organic molecules, $|\boldsymbol{m}|$ is usually much lower than $|\boldsymbol{\mu}|$, so the formula can be

simplified as $g = 4\cos\theta|\boldsymbol{m}|/|\boldsymbol{\mu}|$. Therefore, larger $|\boldsymbol{m}|$ and $\cos\theta$ as well as smaller $|\boldsymbol{\mu}|$ can lead to higher g values. In our case, the $\boldsymbol{\mu}$, $\boldsymbol{m}$, and θ of compounds **1a-c** for their $S_0 \rightarrow S_1$ and $S_0 \rightarrow S_2$ transitions were calculated (Table 1). Theoretical dissymmetry factors ($|g_{cal}|$) of **1a-c** for the $S_0 \rightarrow S_2$ transition were more than one order of magnitude higher than those for the $S_0 \rightarrow S_1$ transition, in good agreement with the experimental results (Table 1). The high $|g_{cal}|$ for the $S_0 \rightarrow S_2$ transition were attributed to the smaller $|\boldsymbol{\mu}|$ and larger $|\boldsymbol{m}|$ compared with those for the $S_0 \rightarrow S_1$ transition, whereas $|\cos\theta|$ equaled to 1 for all cases. Due to the opposite resonance effect of B and N atoms, molecular orbitals on the carbazole segments were well separated between HOMO and LUMO as well as between HOMO and LUMO+1 (Figure 4). However, the orbital distribution on the central benzene was more separated between HOMO and LUMO+1 than that between HOMO and LUMO. Such a smaller overlap integral between HOMO and LUMO+1 could result in lower $|\boldsymbol{\mu}|$ for the $S_0 \rightarrow S_2$ transition, which might contribute to the higher $|g_{cal}|$ values.[46]

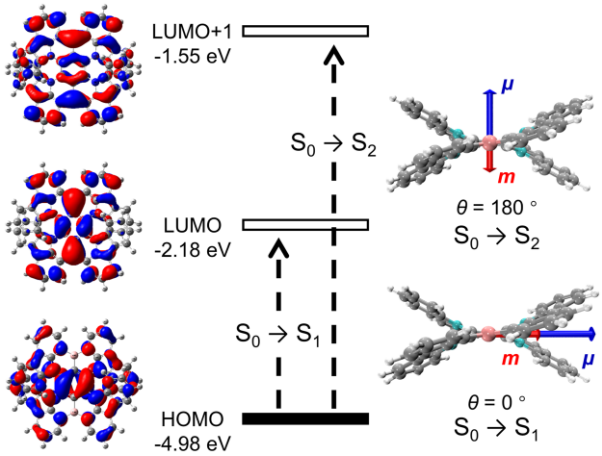

Figure 4. TD-DFT-calculated results of **1a**-(*P*,*P*) with the electric ($\boldsymbol{\mu}$) and magnetic ($\boldsymbol{m}$) transition dipole moments. For clarity, the length of the $\boldsymbol{m}$ vector is amplified 400 and 35 times for the $S_0 \rightarrow S_1$ and $S_0 \rightarrow S_2$ transitions, respectively.

Furthermore, fluorescence and CPL spectra of **1a-c** were characterized to examine their potential as CPL emitters (Figures S1b and S8). Compounds **1a-c** exhibited emission maxima (λ_{em}) at 660 nm, 684 nm, and 694 nm, with high PLQYs of 100%, 99%, and 90%, respectively. Through tuning the peripheral substituents, the fluorescence spectra of **1a-c** extended from the deep-red to the NIR region. Each pair of enantiomers exhibited mirror-image CPL spectra with luminescence dissymmetry factors (g_{lum}) up to 2×10^{-3}, and similar red-shifts as in the fluorescence spectra upon peripheral functionalization (Figure S8). The high PLQYs of compounds **1a-c**, together with their finely tuned emitting properties, make them promising for CPL-related applications.[47]

In summary, we have synthesized the first B,N-embedded double heterohelicenes (**1a-c**) with nonbonded B and N atoms. The excellent configurational stability of the skeleton has enabled successful chiral separation of their enantiomers. Further CD characterization has revealed strong chiroptical responses from 300 to 700 nm, with the maximum $|g_{abs}|$ reaching 0.033 (502 nm), 0.031 (518 nm), and 0.026 (526 nm) for **1a-c**, respectively, representing the highest $|g_{abs}|$ values in the visible range for helicene compounds. Such high $|g_{abs}|$ values has been found to be contributed by the separated HOMO and LUMO+1

induced by the nonbonded B and N atoms. Furthermore, compounds **1a-c** also exhibit CPL activities in the red/NIR regions, with $|g_{lum}|$ up to 0.002 and PLQYs up to 100%. This work has provided a new type of B,N-embedded double heterohelicenes with excellent chiroptical properties, and would stimulate further development of novel helicene-based materials for future chiral optoelectronic applications.

AUTHOR INFORMATION

Corresponding Author

*Email: xiaoye.wang@nankai.edu.cn

Author Contributions

All authors have given approval to the final version of the manuscript.

ACKNOWLEDGMENT

We are grateful to the financial support from the National Natural Science Foundation of China (Nos. 21901128 and 22071120), the National Key R&D Program of China (2020YFA0711500), and the Fundamental Research Funds for the Central Universities. The authors cordially thank Prof. Chuan-Feng Chen and Prof. Meng Li for their kind help on CPL measurements.

Notes

The authors declare no competing financial interest.

REFERENCES

1. Shen, Y.; Chen, C.-F., Helicenes: synthesis and applications. *Chem. Rev.* **2012,** *112*, 1463-1535.
2. Gingras, M., One hundred years of helicene chemistry. Part 1: non-stereoselective syntheses of carbohelicenes. *Chem. Soc. Rev.* **2013,** *42*, 968-1006.
3. Gingras, M.; Félix, G.; Peresutti, R., One hundred years of helicene chemistry. Part 2: stereoselective syntheses and chiral separations of carbohelicenes. *Chem. Soc. Rev.* **2013,** *42*, 1007-1050.
4. Gingras, M., One hundred years of helicene chemistry. Part 3: applications and properties of carbohelicenes. *Chem. Soc. Rev.* **2013,** *42*, 1051-1095.
5. Zhao, W.-L.; Li, M.; Lu, H.-Y.; Chen, C.-F., Advances in helicene derivatives with circularly polarized luminescence. *Chem. Commun.* **2019,** *55*, 13793-13803.
6. Stará, I. G.; Starý, I., Helically Chiral Aromatics: The Synthesis of Helicenes by [2 + 2 + 2] Cycloisomerization of π-Electron Systems. *Acc. Chem. Res.* **2020,** *53*, 144-158.
7. Yang, Y.; da Costa, R. C.; Fuchter, M. J.; Campbell, A. J., Circularly polarized light detection by a chiral organic semiconductor transistor. *Nat. Photonics* **2013,** *7*, 634-638.
8. Zhang, L.; Song, I.; Ahn, J.; Han, M.; Linares, M.; Surin, M.; Zhang, H.-J.; Oh, J. H.; Lin, J., π-Extended perylene diimide double-heterohelicenes as ambipolar organic semiconductors for broadband circularly polarized light detection. *Nat Commun* **2021,** *12*, 142.
9. Wang, L.; Xue, Y.; Cui, M.; Huang, Y.; Xu, H.; Qin, C.; Yang, J.; Dai, H.; Yuan, M., A Chiral Reduced-Dimension Perovskite for an Efficient Flexible Circularly Polarized Light Photodetector. *Angew. Chem. Int. Ed.* **2020,** *59*, 6442-6450.

10. Wang, X.; Wang, Y.; Gao, W.; Song, L.; Ran, C.; Chen, Y.; Huang, W., Polarization-Sensitive Halide Perovskites for Polarized Luminescence and Detection: Recent Advances and Perspectives. *Adv. Mater.* **2021,** *33*, 2003615.
11. Nakai, Y.; Mori, T.; Inoue, Y., Theoretical and Experimental Studies on Circular Dichroism of Carbo[n]helicenes. *J. Phys. Chem. A* **2012,** *116*, 7372-7385.
12. Xiao, X.; Pedersen, S. K.; Aranda, D.; Yang, J.; Wiscons, R. A.; Pittelkow, M.; Steigerwald, M. L.; Santoro, F.; Schuster, N. J.; Nuckolls, C., Chirality Amplified: Long, Discrete Helicene Nanoribbons. *J. Am. Chem. Soc.* **2021,** *143*, 983-991.
13. Qiu, Z.; Ju, C.-W.; Frédéric, L.; Hu, Y.; Schollmeyer, D.; Pieters, G.; Müllen, K.; Narita, A., Amplification of Dissymmetry Factors in π-Extended [7]- and [9]Helicenes. *J. Am. Chem. Soc.* **2021,** *143*, 4661-4667.
14. Schuster, N. J.; Joyce, L. A.; Paley, D. W.; Ng, F.; Steigerwald, M. L.; Nuckolls, C., The Structural Origins of Intense Circular Dichroism in a Waggling Helicene Nanoribbon. *J. Am. Chem. Soc.* **2020,** *142*, 7066-7074.
15. Saal, F.; Zhang, F.; Holzapfel, M.; Stolte, M.; Michail, E.; Moos, M.; Schmiedel, A.; Krause, A. M.; Lambert, C.; Würthner, F.; Ravat, P., [n]Helicene Diimides (n = 5, 6, and 7): Through-Bond versus Through-Space Conjugation. *J. Am. Chem. Soc.* **2020,** *142*, 21298-21303.
16. Liu, B.; Böckmann, M.; Jiang, W.; Doltsinis, N. L.; Wang, Z., Perylene Diimide-Embedded Double [8]Helicenes. *J. Am. Chem. Soc.* **2020,** *142*, 7092-7099.
17. Nakakuki, Y.; Hirose, T.; Sotome, H.; Miyasaka, H.; Matsuda, K., Hexa-*peri*-hexabenzo[7]helicene: Homogeneously π-Extended Helicene as a Primary Substructure of Helically Twisted Chiral Graphenes. *J. Am. Chem. Soc.* **2018,** *140*, 4317-4326.
18. Chen, Y.; Lin, C.; Luo, Z.; Yin, Z.; Shi, H.; Zhu, Y.; Wang, J., Double π-Extended Undecabenzo[7]helicene. *Angew. Chem. Int. Ed.* **2021,** *60*, 7796-7801.
19. Ma, S.; Gu, J.; Lin, C.; Luo, Z.; Zhu, Y.; Wang, J., Supertwistacene: A Helical Graphene Nanoribbon. *J. Am. Chem. Soc.* **2020,** *142*, 16887-16893.
20. Zhu, Y.; Guo, X.; Li, Y.; Wang, J., Fusing of Seven HBCs toward a Green Nanographene Propeller. *J. Am. Chem. Soc.* **2019,** *141*, 5511-5517.
21. Liu, G.; Koch, T.; Li, Y.; Doltsinis, N. L.; Wang, Z., Nanographene Imides Featuring Dual-Core Sixfold [5]Helicenes. *Angew. Chem. Int. Ed.* **2019,** *58*, 178-183.
22. Hu, Y.; Paternò, G. M.; Wang, X.-Y.; Wang, X.-C.; Guizzardi, M.; Chen, Q.; Schollmeyer, D.; Cao, X.-Y.; Cerullo, G.; Scotognella, F.; Müllen, K.; Narita, A., π-Extended Pyrene-Fused Double [7]Carbohelicene as a Chiral Polycyclic Aromatic Hydrocarbon. *J. Am. Chem. Soc.* **2019,** *141*, 12797-12803.
23. Cruz, C. M.; Márquez, I. R.; Castro-Fernández, S.; Cuerva, J. M.; Maçôas, E.; Campaña, A. G., A Triskelion-Shaped Saddle-Helix Hybrid Nanographene. *Angew. Chem. Int. Ed.* **2019,** *58*, 8068-8072.
24. Zhu, Y.; Xia, Z.; Cai, Z.; Yuan, Z.; Jiang, N.; Li, T.; Wang, Y.; Guo, X.; Li, Z.; Ma, S.; Zhong, D.; Li, Y.; Wang, J., Synthesis and Characterization of Hexapole [7]Helicene, A Circularly Twisted Chiral Nanographene. *J. Am. Chem. Soc.* **2018,** *140*, 4222-4226.
25. Schuster, N. J.; Hernández Sánchez, R.; Bukharina, D.; Kotov, N. A.; Berova, N.; Ng, F.; Steigerwald, M. L.; Nuckolls, C., A Helicene Nanoribbon with Greatly Amplified Chirality. *J. Am. Chem. Soc.* **2018,** *140*, 6235-6239.
26. Schuster, N. J.; Paley, D. W.; Jockusch, S.; Ng, F.; Steigerwald, M. L.; Nuckolls, C., Electron Delocalization in Perylene Diimide Helicenes. *Angew. Chem. Int. Ed.* **2016,** *55*, 13519-13523.

27. Evans, P. J.; Ouyang, J.; Favereau, L.; Crassous, J.; Fernández, I.; Perles, J.; Martín, N., Synthesis of a Helical Bilayer Nanographene. *Angew. Chem. Int. Ed.* **2018,** *57*, 6774-6779.
28. Cruz, C. M.; Castro-Fernández, S.; Maçôas, E.; Cuerva, J. M.; Campaña, A. G., Undecabenzo[7]superhelicene: A Helical Nanographene Ribbon as a Circularly Polarized Luminescence Emitter. *Angew. Chem. Int. Ed.* **2018,** *57*, 14782-14786.
29. Fujikawa, T.; Segawa, Y.; Itami, K., Synthesis, Structures, and Properties of π-Extended Double Helicene: A Combination of Planar and Nonplanar π-Systems. *J. Am. Chem. Soc.* **2015,** *137*, 7763-8.
30. Mori, T., Chiroptical Properties of Symmetric Double, Triple, and Multiple Helicenes. *Chem. Rev.* **2021,** *121*, 2373-2412.
31. Dhbaibi, K.; Favereau, L.; Crassous, J., Enantioenriched Helicenes and Helicenoids Containing Main-Group Elements (B, Si, N, P). *Chem. Rev.* **2019,** *119*, 8846-8953.
32. Sun, Z.; Yi, C.; Liang, Q.; Bingi, C.; Zhu, W.; Qiang, P.; Wu, D.; Zhang, F., π-Extended C_2-Symmetric Double NBN-Heterohelicenes with Exceptional Luminescent Properties. *Org. Lett.* **2020,** *22*, 209-213.
33. Maeda, C.; Nagahata, K.; Shirakawa, T.; Ema, T., Azahelicene-Fused BODIPY Analogues Showing Circularly Polarized Luminescence. *Angew. Chem. Int. Ed.* **2020,** *59*, 7813-7817.
34. Full, J.; Panchal, S. P.; Götz, J.; Krause, A.-M.; Nowak-Król, A., Modular Synthesis of Organoboron Helically Chiral Compounds: Cutouts from Extended Helices. *Angew. Chem. Int. Ed.* **2021,** *60*, 4350-4357.
35. Domínguez, Z.; López-Rodríguez, R.; Álvarez, E.; Abbate, S.; Longhi, G.; Pischel, U.; Ros, A., Azabora[5]helicene Charge-Transfer Dyes Show Efficient and Spectrally Variable Circularly Polarized Luminescence. *Chem. Eur. J.* **2018,** *24*, 12660-12668.
36. Hatakeyama, T.; Hashimoto, S.; Oba, T.; Nakamura, M., Azaboradibenzo[6]helicene: carrier inversion induced by helical homochirality. *J. Am. Chem. Soc.* **2012,** *134*, 19600-19603.
37. Shen, C.; Srebro-Hooper, M.; Jean, M.; Vanthuyne, N.; Toupet, L.; Williams, J. A. G.; Torres, A. R.; Riives, A. J.; Muller, G.; Autschbach, J.; Crassous, J., Synthesis and Chiroptical Properties of Hexa-, Octa-, and Deca-azaborahelicenes: Influence of Helicene Size and of the Number of Boron Atoms. *Chem. Eur. J.* **2017,** *23*, 407-418.
38. Wang, X.; Wang, J.; Pei, J., BN Heterosuperbenzenes: Synthesis and Properties. *Chem. Eur. J.* **2015,** *21*, 3528-3539.
39. Zhao, R.; Liu, J.; Wang, L., Polymer Acceptors Containing B←N Units for Organic Photovoltaics. *Acc. Chem. Res.* **2020,** *53*, 1557-1567.
40. Madayanad Suresh, S.; Hall, D.; Beljonne, D.; Olivier, Y.; Zysman-Colman, E., Multiresonant Thermally Activated Delayed Fluorescence Emitters Based on Heteroatom-Doped Nanographenes: Recent Advances and Prospects for Organic Light-Emitting Diodes. *Adv. Funct. Mater.* **2020,** *30*, 1908677.
41. Zhuang, F.; Sun, Z.; Yao, Z.; Chen, Q.; Huang, Z.; Yang, J.; Wang, J.; Pei, J., BN-Embedded Tetrabenzopentacene: A Pentacene Derivative with Improved Stability. *Angew. Chem. Int. Ed.* **2019,** *58*, 10708-10712.
42. Yang, M.; Park, I. S.; Yasuda, T., Full-Color, Narrowband, and High-Efficiency Electroluminescence from Boron and Carbazole Embedded Polycyclic Heteroaromatics. *J. Am. Chem. Soc.* **2020,** *142*, 19468-19472.
43. During the preparation of this manuscript, Zhang and Duan et al. reported relevant compounds (**1a**,**b**) as deep-red emitters for highly efficient organic light-emitting diodes (published on July 28th). However, no chiroptical properties were investigated, which distinguishes the current work from their contribution. See: Zhang, Y.; Zhang, D.; Huang, T.; Gillett, A. J.; Liu, Y.; Hu, D.; Cui, L.; Bin, Z.; Li, G.; Wei, J.; Duan,

L., Multi-Resonance Deep-Red Emitters with Shallow Potential-Energy Surfaces to Surpass Energy-Gap Law. *Angew. Chem. Int. Ed.* **2021,** DOI: 10.1002/anie.202107848.
44. Hatakeyama, T.; Shiren, K.; Nakajima, K.; Nomura, S.; Nakatsuka, S.; Kinoshita, K.; Ni, J.; Ono, Y.; Ikuta, T., Ultrapure Blue Thermally Activated Delayed Fluorescence Molecules: Efficient HOMO-LUMO Separation by the Multiple Resonance Effect. *Adv. Mater.* **2016,** *28*, 2777-2781.
45. Tanaka, H.; Ikenosako, M.; Kato, Y.; Fujiki, M.; Inoue, Y.; Mori, T., Symmetry-based rational design for boosting chiroptical responses. *Commun. Chem.* **2018,** *1*, 38.
46. Kubo, H.; Hirose, T.; Nakashima, T.; Kawai, T.; Hasegawa, J.-y.; Matsuda, K., Tuning Transition Electric and Magnetic Dipole Moments: [7]Helicenes Showing Intense Circularly Polarized Luminescence. *J. Phys. Chem. Lett.* **2021,** *12*, 686-695.
47. Zhang, D.-W.; Li, M.; Chen, C.-F., Recent advances in circularly polarized electroluminescence based on organic light-emitting diodes. *Chem. Soc. Rev.* **2020,** *49*, 1331-1343.